Generation of optical frequency comb squeezed light field with TEM$_{01}$ transverse mode

Nan Huo (霍 楠)[1,2], **Chihua Zhou (周驰华)**[1,2], **Hengxin Sun (孙恒信)**[1,2],
Kui Liu (刘 奎)[1,2,*], **and Jiangrui Gao (郜江瑞)**[1,2]

[1]*State Key Laboratory of Quantum Optics and Quantum Optics Devices, Institute of Opto-Electronics,
Shanxi University, Taiyuan 030006, China*
[2]*Collaborative Innovation Center of Extreme Optics, Shanxi University, Taiyuan 030006, China*
Corresponding author: liukui@sxu.edu.cn
Received February 2, 2016; accepted April 15, 2016; posted online May 20, 2016

Nonclassical optical frequency combs find tremendous utility in quantum information and high-precision quantum measurement. The characteristics of a type-I synchronously pumped optical parametric oscillator with the TEM$_{01}$ transverse mode below threshold are investigated and a squeezing of 0.7 dB for an optical frequency comb squeezed light field with the TEM$_{01}$ transverse mode is obtained under the pump power of 130 mW. This work has a promising application in three-dimensional space-time measurement.

OCIS codes: 270.6570, 190.4410, 190.7110.
doi: 10.3788/COL201614.062702.

Optical frequency combs, which span over thousands of different frequency modes, have found tremendous utility in precision measurement[1–5] and quantum information[6,7]. In 2008, Fabre *et al.* put forward a new scheme combining a balanced homodyne detector (BHD) with mode-locked ultrafast frequency combs that lead to a new shot noise limit (SNL) in time transfer and demonstrated that the time measurement precision is enhanced by taking advantage of the nonclassical optical frequency combs as the signal field[8]. Then this team experimentally prepared a spatially fundamental mode nonclassical frequency comb for the first time and obtained -1.2 ± 0.1 dB of the amplitude squeezing[9]. Recently, they have realized wavelength-multiplexed quantum networks and a quantum spectrometer based on the nonclassical optical frequency combs[10,11].

Spatial transverse modes own a more complex spatial structure and more information, thus allowing parallel transfer of quantum information through an optical network[12]. Combining the respective advantages of optical frequency combs and spatial high-order transverse modes, the quantum network that contains a greater channel capacity can be achieved by using wavelength division multiplexing and space division multiplexing[13,14]. In addition, high-order transverse mode nonclassical optical frequency combs will hopefully be used in three-dimensional (3D) space-time measurements.

In 2013, our group observed -2.58 dB of the phase quadrature squeezing of the TEM$_{00}$ mode by a type-I degenerate synchronously pumped optical parametric oscillator (SPOPO) that operated below its oscillation threshold[15]. In the present work, we obtained the amplitude quadrature squeezing of -0.7 dB by the use of the SPOPO that operated in a high-order transverse mode state. This work has had a profound effect on the quantum network and space-time precision measurement.

Considering a process in which the femtosecond pulse laser with center frequencies 2ω pumping the SPOPO with a type-I nonlinear crystal is converted into a downconversion field at frequencies around ω, the interaction Hamiltonian for a type-I SPOPO is expressed by[16]

$$\hat{H}_I = i \sum_{j,q,m} \chi_{j,q,m} f_{q,m}^j a_q(t) a_m(t) \hat{p}_j(t) + \text{H.c.}, \qquad (1)$$

where $\hat{a}_k$ $(k = m, q)$ are annihilation operators of the downconversion fields with frequency $\omega + k\Omega$, $\hat{p}_j$ $(j = m + q)$ is an annihilation operator of the pump field with frequency $2\omega + j\Omega$, and Ω is the free spectral range of the SPOPO and equal to the repetition of the pumping laser. $f_{q,m}^j$ is the phase-mismatch factor, because the femtosecond pulse has a spectral width of several nanometers, the perfect phase matching is achieved only at the center frequency. $\chi_{j,q,m}$ is the nonlinear coupling constant; it is dependent on the spatial overlap between the pump and the downconversion fields and read as

$$\chi_{j,q,m} \approx \chi^{(2)} A_{I01} = \chi^{(2)} \iint u_j u_m^* u_q^* \mathrm{d}x\mathrm{d}y, \qquad (2)$$

where u_j and u_k $(k = m, q)$ are the transverse distribution of the pump field and the downconversion fields, respectively, $\chi^{(2)}$ is the second-order susceptibility of the nonlinear crystal in the center frequency, and A_{I01} is the interaction area. In our experimental scheme, the downconversion fields are operated in the TEM$_{01}$ transverse mode and the pump field is in the TEM$_{00}$ transverse mode. We can get $\chi_{j,q,m} = \chi_0/2$, which is much smaller than the nonlinear coupling constant χ_0 between the TEM$_{00}$ pump field and the TEM$_{00}$ downconversion fields[17,18].

Assuming that the pump field is not depleted, the pump annihilation operator is approximated as $\langle \hat{p}_j(t) \rangle \approx \varepsilon \alpha_j$, ε is

the electric average amplitude of the pump field including all of the longitudinal modes, and α_j is the normalized longitudinal mode weight. The Langevin equation of the intracavity field is expressed as

$$\frac{\mathrm{d}\hat{a}_m}{\mathrm{d}t} = -\gamma\hat{a}_m - \gamma\sigma\sum_q f_{q,m}^j\alpha_j\hat{a}_q + \sqrt{2\gamma_s}\hat{a}_{\mathrm{in},m} + \sqrt{2\gamma_\nu}\hat{a}_{\nu,m},\tag{3}$$

where $\gamma = \gamma_s + \gamma_\nu$ is the total decay rate, γ_s and γ_ν are the resonant decay rates corresponding to the input coupler and the vacuum input coupler, respectively; $\sigma = \varepsilon/\varepsilon_{\mathrm{th}}^{01}$ is a coupling constant, and $\varepsilon_{\mathrm{th}}^{01} = \gamma/\chi_{j,q,m}$ denotes the continuous wave (CW) pump threshold of a simple-mode optical parameter oscillator (OPO) operating in the TEM_{01} transverse mode[16].

The mode-locked femtosecond pulse laser exports pulse trains on the order of 10^4–10^5, so the downconversion process in the SPOPO is a very complicated multimode interaction process. This nonlinear interaction is taken as a multimode correlation, and it can be transformed into a single-mode squeezed state by the Bloch–Messiah reduction[19]. In the SPOPO, squeezing is not effective in a single-frequency mode, as usual, but instead in a whole set of "super modes"[20], which are well-defined linear combinations of signal modes of different frequencies. Likewise, super mode $\hat{S}_m(t)$ satisfies the Langevin equation:

$$\frac{\mathrm{d}}{\mathrm{d}t}\hat{S}_m = -\gamma\hat{S}_m - \gamma\sigma\Lambda_m\hat{S}_m + \sqrt{2\gamma_s}\hat{S}_{\mathrm{in},m} + \sqrt{2\gamma_\nu}\hat{S}_{\nu,m},\tag{4}$$

where $\hat{S}_m(t) = \sum_q L_{m,q}\hat{s}_q(t)$, $L_{m,q}$ is the coefficient of coupling different frequency signal modes, and Λ_m is denoted as the squeezed level of the mth super mode.

After the Fourier transformation, the quantum fluctuation of the output of the SPOPO is calculated as follows:

$$\delta^2\tilde{S}_{\mathrm{out},m}^{(\pm)}(\omega) = \frac{\gamma_s^2(1\mp r\Lambda_m/\Lambda_0)^2 + \omega^2}{\gamma^2(1\pm r\Lambda_m/\Lambda_0)^2 + \omega^2},\tag{5}$$

where $\hat{S}^{(+)} = \hat{S} + \hat{S}^\dagger$ and $\hat{S}^{(-)} = -i(\hat{S} - \hat{S}^\dagger)$ are the amplitude and phase quadrature of the super mode, respectively, $r = \varepsilon/\varepsilon_{\mathrm{th}}$ is the normalized amplitude pumping rate, and $\varepsilon_{\mathrm{th}} = \varepsilon_{\mathrm{th}}^{01}/\Lambda_0$[16] ($\Lambda_0$ is about 220) is the threshold of the SPOPO and is extremely lower than the threshold of a single-mode OPO.

In our experiment, we only measured the quantum fluctuation of the output fields with temporal zero-order super modes and spatial TEM_{01} transverse modes. Taking the loss and the efficiency into consideration, the quadrature amplitude noise power was written as[21]

$$\delta^2\tilde{S}_{\mathrm{out}}^{(+)}(\omega) = 1 - \eta_{\mathrm{total}}\rho\frac{4r}{(1+r)^2 + (\omega/\gamma)^2},\tag{6}$$

where $\eta_{\mathrm{total}} = \varsigma\eta\xi$ is the total detection efficiency and $\rho = \gamma_s/\gamma$ stands for the escape efficiency.

The schematic of the experimental setup is shown in Fig. 1. A Ti:sapphire mode-locked laser (Coherent Mira900) pumped by an Nd:YVO$_4$ laser (Coherent Verdi18) at 532 nm produced 130 fs pulse trains at 850 nm with a repetition rate of 76 MHz. These trains were divided into two parts; most of the light passed the second harmonic generator (SHG), which produced the pump field at 425 nm to pump the SPOPO. The remaining part was broken into two parts by a beam splitter (BS); half of the light was injected into the SPOPO as the seed beam, the other half entered into the mode cleaner and generated the local oscillator field of the BHD[22]. The output of the SPOPO entered into the BHD and was analyzed by a spectrum analyzer (SA).

In the SPOPO, a length of 300 μm of the PPKTP crystal is taken as a nonlinear medium. The cavity of the SPOPO includes two concave mirrors M2 and M3 with 30 cm curvature radii and two plane mirrors M1 and M4. M1 is used as the input coupling mirror, which is highly reflective at 850 nm and antireflective at 425 nm; M4 is the output coupling mirror, which is highly reflective at 425 nm and has a transmittance of $T = 20\%$ at 850 nm. The length of the round trip is about 4 m, which is as long as the resonant cavity of the laser. The mode cleaner, which has the same free spectral regime as the SPOPO, consists of two concave mirrors with 30 cm curvature radii and four plane mirrors. In the mode cleaner, two concave mirrors are highly reflective at 850 nm; the input mirror and the output mirror all have a transmittance of $T = 10\%$ at 850 nm.

In our experiment, we introduced a small tilt in the front of the SPOPO to produce the TEM_{01} mode as the signal field[23,24]. Meanwhile, the Hansch–Couillaud locking method was used to lock the cavity length in order to export the stable signal fields[25]. Before the interaction, the matching between the pump field and the seed beam needed to meet two conditions, i.e., spatial overlap and time synchronization. In order to meet these two conditions, the seed beam singly passed the nonlinear crystal and the generated second harmonic beam interfered with the pump field; at the same time, we also added the delay line in the light path. Under the pump power of 130 mW, the classical gain of the TEM_{01} mode was 2. When the
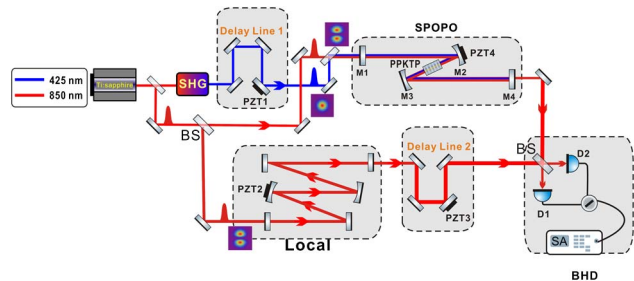

Fig. 1. Experimental setup. PZT: piezoelectric ceramic transducer.

relative phase between the seed beam and the pump field was controlled in the deamplification regime, the noise of the output field was measured by the BHD. In order to match the local oscillator with the signal field, the local oscillator with a temporal zero-order super mode and spatial TEM_{01} transverse mode was selected by the mode cleaner.

The noise of the input signal field has an influence on the measurement of the squeezed state. We first measured the noise of the input signal field that was directly output from the laser, as shown in Fig. 2. The blue (dashed) line is the electronic noise, the black (dotted) line is the SNL, and the red (solid) line is the input signal field noise. It can be seen from Fig. 2 that our detection system has a good response above 0.5 MHz and is able to detect the squeezing. The noise of input signal field reaches the SNL after 1.2 MHz, but the signal field has a large extra noise below 1.2 MHz, which will drown out the squeezing of the output field. In addition, from Eq. (6), we can see that the lower the analysis frequency is the higher the squeezing is, so the analysis frequency should be as small as possible. Based on the analysis, we detected the squeezing of the output field at the analysis frequency of 1.2 MHz.

The measurement results are shown in Fig. 3 at the analysis frequency of 1.2 MHz and the measurement parameters of the SA with a resolution bandwidth (RBW) of 470 kHz and a video bandwidth (VBW) of 180 Hz. We first calibrated the SNL (blue solid line), and next we measured the noise traces for the output field while the phase (PZT3) of the local field was scanned. From the measured data, we find -0.7 dB of the amplitude quadrature squeezing.

The measured squeezing values were degraded by the various inefficiencies of our setup. We estimated this efficiency $\eta_{\text{total}} = \varsigma \eta \xi$, where $\varsigma = 78\%$ was the measured propagation efficiency, $\eta = 85\%$ was the measured photodiode (Hamamatsu S5971) quantum efficiency, and $\xi = 87\%$ was the interference visibility between the local
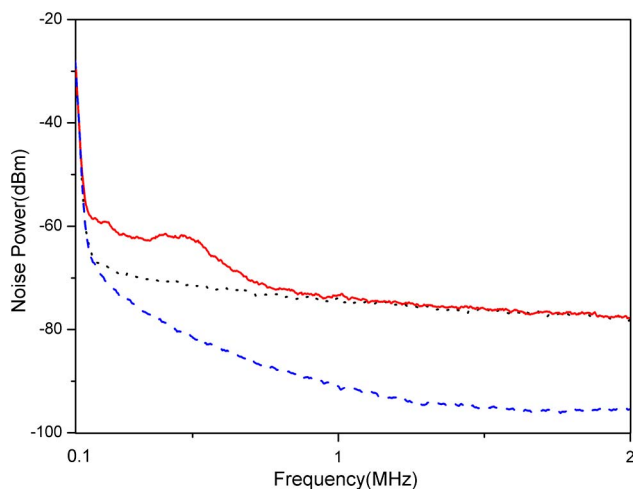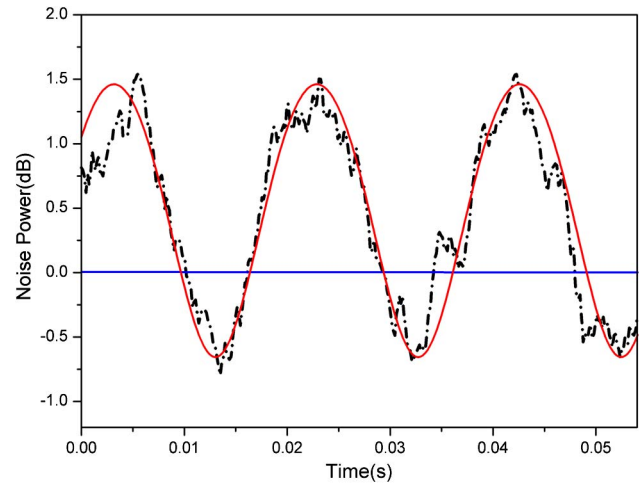

Fig. 3. Amplitude squeezing of the TEM_{01} transverse mode versus the sweeping time. The black dotted lines are the experimental plots while the red solid lines are their fittings.

oscillator (280 µW) and the signal field (10.3 µW). The total estimated detection efficiencies for our experiment were therefore $\eta_{\text{total}} = 57.6\%$. From these efficiencies, the inferred amplitude squeezing was -2.3 dB.

In Fig. 3, the noise power lines flutter severely because the long distance reduces the stability of the system. The squeezed degree of the high-order transverse mode is lower than that of the fundamental transverse mode because the optimal pump transverse mode should be a superposition of the TEM_{00} mode and the TEM_{02} mode[12].

In conclusion, we experimentally demonstrate an optical frequency comb squeezed light field with a TEM_{01} transverse mode in the SPOPO. Considering experimental measurement efficiency, we infer that the amplitude squeezing is -2.3 dB. Nevertheless, the squeezing is still relatively low due to the extra losses and various inefficiencies in our experiment. In addition, the pump transverse mode is not in an optimized spatial profile, leading to the low downconversion efficiency. This work is significant in quantum networks and space-time precision measurement.

References

1. Th. Udem, R. Holzwarth, and T. W. Hänsch, Nature **416**, 233 (2002).
2. T. Rosenband, D. B. Hume, P. O. Schmidt, C. W. Chou, A. Brusch, L. Lorini, W. H. Oskay, R. E. Drullinger, T. M. Fortier, J. E. Stalnaker, S. A. Diddams, W. C. Swann, N. R. Newbury, W. M. Itano, D. J. Wineland, and J. C. Bergquist, Science **319**, 1808 (2008).

Fig. 2. Noise of the input signal field.

3. X. Jia, Y. Yuan, D. Yang, T. Jia, and Z. Sun, Chin. Opt. Lett. **12**, 113203 (2014).

4. K. Zhai, Z. Li, H. Xie, C. Jing, G. Li, B. Zeng, W. Chu, J. Ni, J. Yao, and Y. Chen, Chin. Opt. Lett. **13**, 050201 (2015).

5. B. Pan, L. Yu, L. Guo, L. Zhang, D. Lu, X. Chen, Y. Wu, C. Lou, and L. Zhao, Chin. Opt. Lett. **14**, 030604 (2016).

6. P. Wang, M. Chen, N. C. Menicucci, and O. Pfister, Conf. Lasers Electro–Opt. **90**, 1 (2014).

7. S. A. Van den Berg, S. T. Persijn, G. J. P. Kok, M. G. Zeitouny, and N. Bhattacharya, Phys. Rev. Lett. **108**, 183901 (2012).

8. B. Lamine, C. Fabre, and N. Treps, Phys. Rev. Lett. **101**, 123601 (2008).

9. O. Pinel, P. Jian, R. M. Arau, J. X. Feng, B. Chalopin, C. Fabre, and N. Treps, Phys. Rev. Lett. **108**, 083601 (2012).

10. J. Roslund, R. M. Arau, S. F. Jiang, C. Fabre, and N. Treps, Nat. Photonics **8**, 109 (2013).

11. Y. Cai, X. Y. Xu, and N. Treps, *Quantum Coherent Control with an Optical Frequency Comb* (Laboratoire Kastler Brossel, 2015).

12. M. Lassen, V. Delaubert, C. C. Harb, P. K. Lam, N. Treps, and H. A. Bachor, JEOS RP **1**, 06003 (2006).

13. A. Ciurana, J. M. Mateo, M. Peev, A. Poppe, N. Walenta, H. Zbinden, and V. Martin, Opt. Express **22**, 1576 (2014).

14. A. V. Zelst, Electrotechnical Conf. **3**, 1218 (2000).

15. H. Y. Liu, L. Chen, L. Liu, Y. Ming, K. Liu, J. X. Zhang, and J. R. Gao, Acta Phys. Sin. **62**, 164206 (2013).

16. G. Patera, N. Treps, C. Fabre, and G. J. Valcarcel, Eur. Phys. J. D **56**, 123 (2010).

17. N. C. Benlloch, G. J. Valcarcel, and E. Roldan, Phys. Rev. A **79**, 043820 (2009).

18. L. Liu, N. Huo, K. Liu, J. X. Zhang, and J. R. Gao, Acta Sinica Quantum Optica **20**, 124 (2014).

19. S. L. Braunstein, Phys. Rev. A **71**, 055801 (2005).

20. G. J. Valcarcel, G. Patera, N. Treps, and C. Fabre, Phys Rev. A **74**, 061801 (2006).

21. T. Aoki, G. Takahashi, and A. Furusawa, Opt. Express **14**, 6930 (2006).

22. K. Liu, S. Z. Cui, H. L. Zhang, J. X. Zhang, and J. R. Gao, Chin. Phys. Lett. **28**, 074211 (2011).

23. T. L. Hsu, W. P. Bowen, N. Treps, and P. K. Lam, Phys. Rev. A **72**, 013802 (2005).

24. H. X. Sun, K. Liu, Z. L. Liu, P. L. Guo, J. X. Zhang, and J. R. Gao, Appl. Phys. Lett. **104**, 121908 (2014).

25. T. W. Hansch and B. Couillaud, Opt. Commun. **35**, 441 (1980).